

# Graphical 3D Visualization of Highway Bridge Ratings

Gregory Esch<sup>1</sup>; Michael H. Scott, A.M.ASCE<sup>2</sup>; and Eugene Zhang<sup>3</sup>

**Abstract:** Aging highway infrastructure requires effective rating methodologies to prioritize bridges for rehabilitation and repair. To aid engineers in decision making regarding bridge maintenance, a three-dimensional (3D) visualization system is developed for rating reinforced concrete deck-girder bridge. Color codings show the most probable mode of failure for girder cross sections under combined moment-shear forces and allow an engineer to determine a rehabilitation strategy. The visualization system relies on 3D finite-element analyses using the open source framework OpenSees, making the system readily extensible to a wide range of bridge types and loading scenarios, as well as emergent reliability-based rating methodologies. Important features of the visualization system are emphasized, including the use of lighting and feature edge detection to improve the visual quality of a bridge model. Recent developments in scientific visualization are discussed for potential application to civil engineering problems.

**DOI:** 10.1061/(ASCE)0887-3801(2009)23:6(355)

**CE Database subject headings:** Bridge management; Maintenance; Computer aided simulation; Graphic methods; Computer programming; Loading rates; Structural analysis; Bridge, highway.

## Introduction

Three-dimensional (3D) visualization has become a powerful analysis and assessment tool in all stages of architecture, engineering, and construction (AEC) of civil infrastructure systems. Visualization of the entire AEC process allows architects, engineers, and contractors to deliver constructed facilities in an efficient and cost-effective manner (Kamat and Martinez 2001). Moreover, with infrastructure systems nearing the end of their originally intended design lives, it is anticipated that 3D visualization will play an increasingly important role as engineers are tasked with evaluation for system repair or replacement. For example, inspections of 1,800 conventionally reinforced concrete deck-girder (RCDG) bridges built in Oregon during the interstate boom of the 1950's revealed that approximately 500 exhibited varying levels of diagonal cracking [Oregon Department of Transportation (ODOT) 2002]. Such symptoms of an aging infrastructure are not unique to the state of Oregon, where a research program was launched to prioritize the affected bridges for repair (Higgins et al. 2004).

Load rating is the primary means by which engineers assess the remaining capacity of highway bridges to carry vehicle loading. While any structural component of a bridge can be rated, particular attention is paid to girders as they transmit loads from

the deck to the supports via shear and flexure. Evaluation methods for girder moment-shear interaction summarized in Fig. 1 include the load and resistance factor rating (LRFR) framework (AASHTO 2003; Minervino et al. 2004) and reliability-based approaches (Stewart et al. 2001) for moment and shear, individually [Figs. 1(a and b)], as well as reliability-based approaches for combined moment-shear effects (Higgins et al. 2005) [Fig. 1(c)]. Rating factors, or alternatively reliability indices (Akgül and Frangopol 2004), allow engineers to determine if a bridge meets an acceptable level of safety.

The objective of this paper is to demonstrate a 3D visualization system for load rating RCDG highway bridges that will allow engineers to determine which structural components are in need of repair and to convey this information effectively to interested stakeholders. The paper begins with an overview of the software design for the rating visualization system, which consists of three parts: container classes for bridge information, a graphical user interface (GUI), and a finite-element analysis engine. This is followed by a discussion of methods the system employs to enhance the quality of the bridge visualization, namely, lighting and feature edge detection. The paper concludes with a discussion of emerging techniques of scientific visualization that merit investigation for civil engineering applications.

## Analysis and Rating Approach

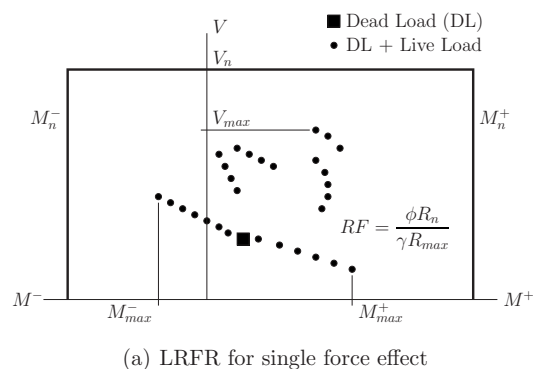
The rating visualization system presented herein is based on the evaluation method shown in Fig. 1(c) for moment-shear interaction; however, any of the methods shown in Fig. 1 could be used. The reliability index,  $\beta$ , indicates the number of standard deviations that separates the peak vehicle-imposed moment-shear force effect from the nominal capacity (Higgins et al. 2005). The capacity curve is calculated using a statistical model of combined moment-shear resistance in reinforced concrete girders (Turan et al. 2008). Load effects of bridge self-weight and vehicle live load are calculated by linear-elastic 3D static analysis with shell elements in the deck connected to girder beam elements via rigid links (Scoggins 2007). Alternative 3D finite-element modeling

<sup>1</sup>Graduate Research Assistant, School of Electrical Engineering and Computer Science, Oregon State Univ., Corvallis, OR 97331. E-mail: eschgr@eecs.oregonstate.edu

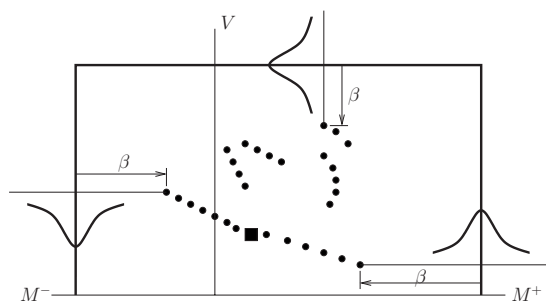
<sup>2</sup>Assistant Professor, School of Civil and Construction Engineering, Oregon State Univ., Corvallis, OR 97331 (corresponding author). E-mail: michael.scott@oregonstate.edu

<sup>3</sup>Assistant Professor, School of Electrical Engineering and Computer Science, Oregon State Univ., Corvallis, OR 97331. E-mail: zhang@eecs.oregonstate.edu

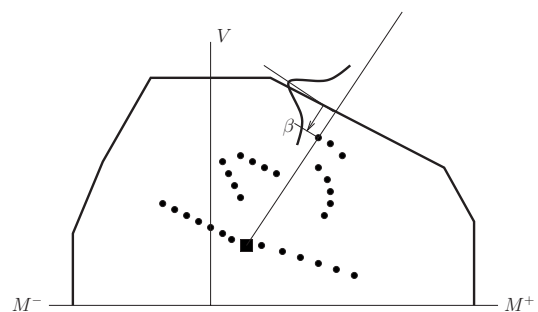
Note. This manuscript was submitted on December 5, 2007; approved on February 9, 2009; published online on October 15, 2009. Discussion period open until April 1, 2010; separate discussions must be submitted for individual papers. This paper is part of the *Journal of Computing in Civil Engineering*, Vol. 23, No. 6, November 1, 2009. ©ASCE, ISSN 0887-3801/2009/6-355-362/\$25.00.



(a) LRFR for single force effect



(b) Reliability-based approach for single force effect



(c) Reliability-based approach for combined force effect

**Fig. 1.** Evaluation methods for bridge girder rating: (a) LRFR for single force effect; (b) reliability-based method for single force effect; (c) reliability-based method for combined force effect

techniques that enforce displacement compatibility of bridge deck-girder systems have been summarized by Chung and Sotolino (2006). Configurations of axle weights for rating vehicles, e.g., special permit trucks [Oregon Department of Transportation (ODOT) 2004], are incrementally moved longitudinally and transversely across the bridge deck and the moment-shear interaction is recorded at each girder cross section of interest for each increment.

Structural analyses for the purposes of bridge rating are carried out using the OpenSees software framework (McKenna et al. 2000), which is a collection of C++ classes that encapsulate the basic building blocks of the finite-element method (Hughes 1987; Bathe 1996; Zienkiewicz and Taylor 2000). To avoid potentially long compilations, model building and analysis commands are added to the Tcl programming language (Ousterhout 1994). This allows users of OpenSees to quickly construct customized applications by composing sequences of OpenSees/Tcl commands into scripts that can be called from a GUI using the C-programming interface of Tcl (Welch 2000). From a development perspective, the scripts provide a layer of abstraction that decouples a GUI from the underlying numerical abstractions of the finite-element

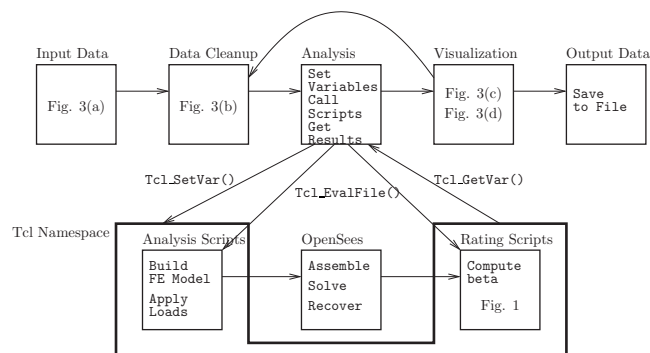


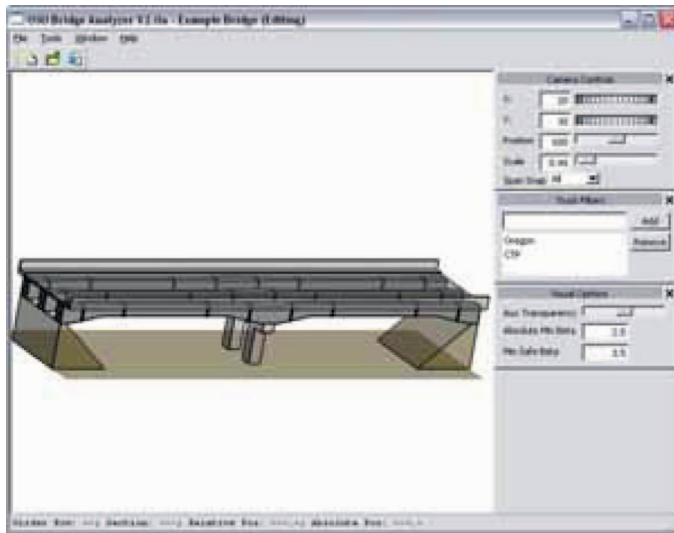
**Fig. 2.** Flowchart showing interaction of major components in bridge rating application

analysis, thereby making OpenSees suited to a wide range of applications not considered in its initial design, e.g., sketching finite-element models (Hutchinson et al. 2007).

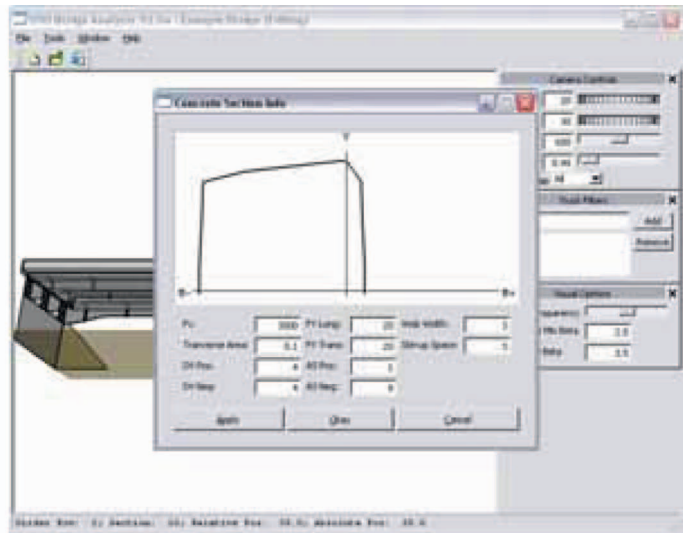
The approach taken in this paper is to create parameterized Tcl scripts to analyze highway bridges for moving vehicle loads in order to rate bridge girders for moment-shear effects. The script parameters are populated and the scripts are executed using the Tcl C-programming interface functions `Tcl_SetVar` and `Tcl_EvalFile`, respectively. Separate scripts encapsulate the 3D finite-element model building, moving load analysis, and rating calculations. This allows a user to make changes to the scripts without recompiling the GUI and visualization components of the system. Analysis and rating results are retrieved from the Tcl namespace using the `Tcl_GetVar` function.

The flow of data through the bridge rating visualization system is shown in Fig. 2 while Fig. 3 captures an accompanying set of images for a typical user-work scenario. The interface shown in Fig. 3 was developed with the Fox Toolkit (van der Zijp 2007), which offers a wider range of widgets than Tk, the Tcl-native GUI framework. Bridge geometry and reinforcing details of girder cross sections identified as critical for rating (based on design drawings and/or field inspection) are entered via a text input file in the “input data” stage, then sent to the GUI for viewing, as shown in Fig. 3(a), or editing by the user in the “data cleanup” stage [Fig. 3(b)]. The “analysis” phase consists of calling the aforementioned Tcl C-programming functions to invoke OpenSees for structural analysis and to obtain rating results, which are then shown to the user in the “visualization” phase. In this phase, the system provides a 3D rendering of the bridge rating, as well as aggregate and segregate 2D views of each girder line, as shown in Figs. 3(c and d), respectively. The bridge can be analyzed again by returning to the data cleanup stage or a text-based summary of the rating information can be given to the user in the “output data” phase.

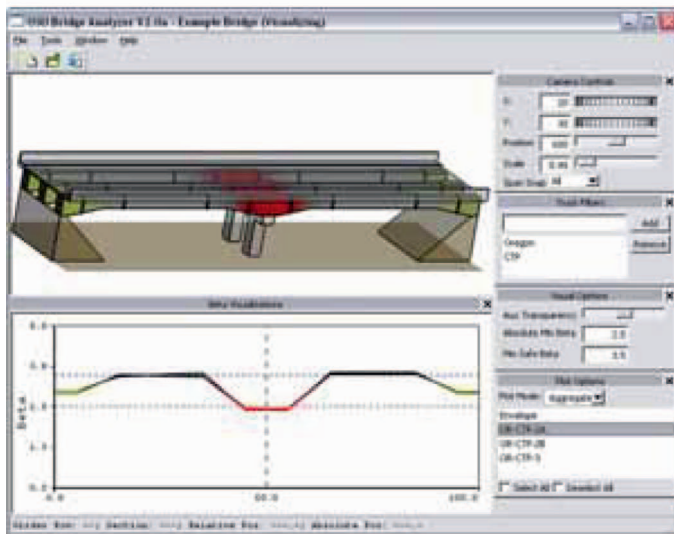
The data required for visualization and analysis in the data cleanup, analysis, and visualization stages are stored in the hierarchy of container classes shown in Fig. 4, which conveys the class relationships using standard UML notation (Booch et al. 1998). The abstract `BridgeComponent` class provides an interface for operations common to all components of a bridge: deck, bents, spans, girders, and sections. To send variables between the container classes and the Tcl namespace, the `loadData()` and `ratingCalc()` methods accept a pointer to a Tcl interpreter object. The `Bridge` container class iterates over its deck, bents, and spans to perform visualization, analysis, and rating operations. A `BridgeSpan` invokes similar operations on its girders and sections.



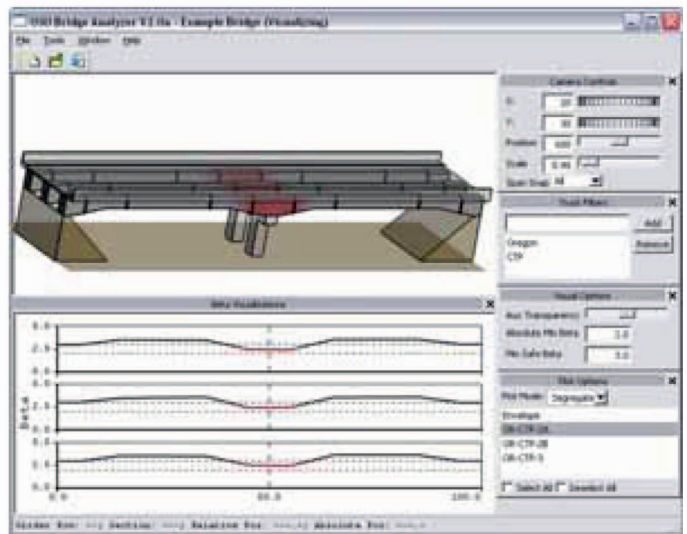
(a) Input bridge properties



(b) Modify section properties



(c) Visualize rating (aggregate)



(d) Visualize rating (segregate)

**Fig. 3.** (Color) Sequence of images showing the user work flow: (a) the user loads a bridge; (b) modifies section properties; (c) and (d) visualizes rating

This iteration allows the system to perform rating calculations over all bridge components as part of a more comprehensive bridge evaluation methodology without significant changes in the underlying software architecture. With the description of the analysis and rating methodology complete, attention now turns to rendering a 3D bridge model in order to visualize analysis and rating results.

### Bridge Visualization Approach

The rating system uses the OpenGL API (Shreiner et al. 2007) for rendering a 3D bridge model. OpenGL was chosen for its excellent performance, ease of use, support for multiple platforms, and extensibility. The bridge visualization technique is based on the Focus+Context approach (Stasko and Zhang 2000), where the user can view and modify bridge properties in a 3D display. This

allows the user to modify reinforcing details at critical girder cross sections before performing the bridge rating calculations, e.g., as shown in the inset of Fig. 3(b). The selection of a critical section on the 3D bridge model is based on a ray to bounding box hierarchy intersection method (Gottschalk et al. 1996).

### Bridge Mesh

For visualization, the bridge is represented by an underlying triangular mesh of vertices, edges, and faces, which does not correspond to the finite-element mesh used for analysis. The system treats each structural component of the bridge separately, which allows components to be reused for different bridge types, e.g., steel girder bridges and to render nonstructural components such as traffic markings if desired. To account for possible tapers and haunches, the RCDG girders considered in this paper are generated by extrusion using cross section dimensions specified by the

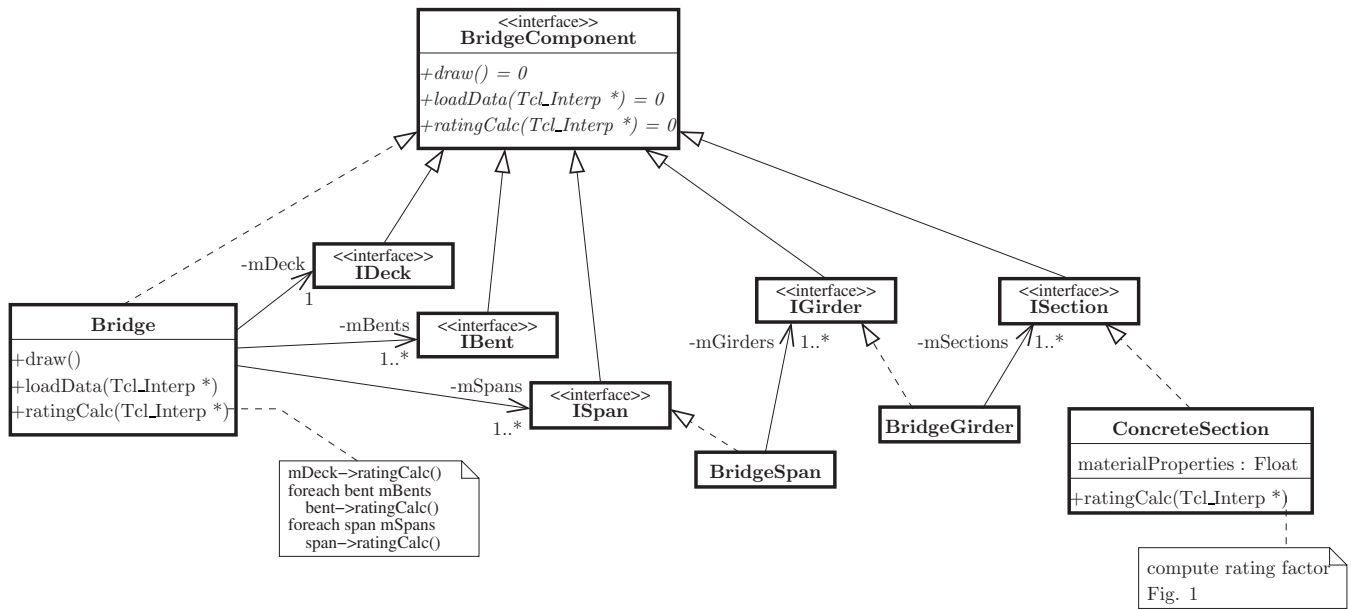


Fig. 4. UML diagram of container classes for visualization and bridge rating

user. The mesh generation is straightforward since it is based locally to a bridge component and does not use dimension information from other components. This local extrusion process makes it easy to change how a bridge component is rendered without affecting the visualization of neighboring components. The deck and bents are generated by scaling of basic shapes. The resulting base mesh is shown in Fig. 5(a).

Once the bridge mesh has been generated from the input file, it must be displayed in a way that exposes the bridge geometry and features. The most basic approach is to draw each structural component of the bridge using solid colors, as shown in Fig. 5(b); however, this results in a flat appearance of the bridge. As described in the following sections, lighting and feature edge detection can be used to provide significant improvements in the visual quality of Fig. 5(b).

### Lighting

The visualization system employs the Phong illumination model (Foley et al. 1996), which considers ambient, diffuse, and specular effects caused by lights. This well-developed model is natively supported in OpenGL and most graphics hardware. Specular effects are disabled to convey the prismatic shape of the bridge components effectively. In the Phong illumination model, a set of materials coincide with the surfaces to describe color properties. Lighting material properties are chosen to match the colors of the construction materials common to concrete bridges. Structural components, such as the girders, bents, and the deck, are colored gray to match the natural color of concrete. The end supports, which are modeled as earthen embankments, are colored brown. Finally, girder cross sections identified as critical for rating are colored blue so that they stand out to the user.

Two directional lights are used to provide a convincing approximation of light originating from a source infinitely far from the bridge. This has the effect of uniformly lighting every part of the bridge surface having the same normal vector. The two lights are set to an intensity of gray, preventing white washing or oversaturation of the rendered image. One directional light is held constant with respect to the camera while the other is held con-

stant with respect to the bridge. This exposes several features of the bridge that were hidden when applying color only, e.g., by giving the user a clearer impression of the tapers and haunches of nonprismatic girders. This is shown in Fig. 5(c), where shading

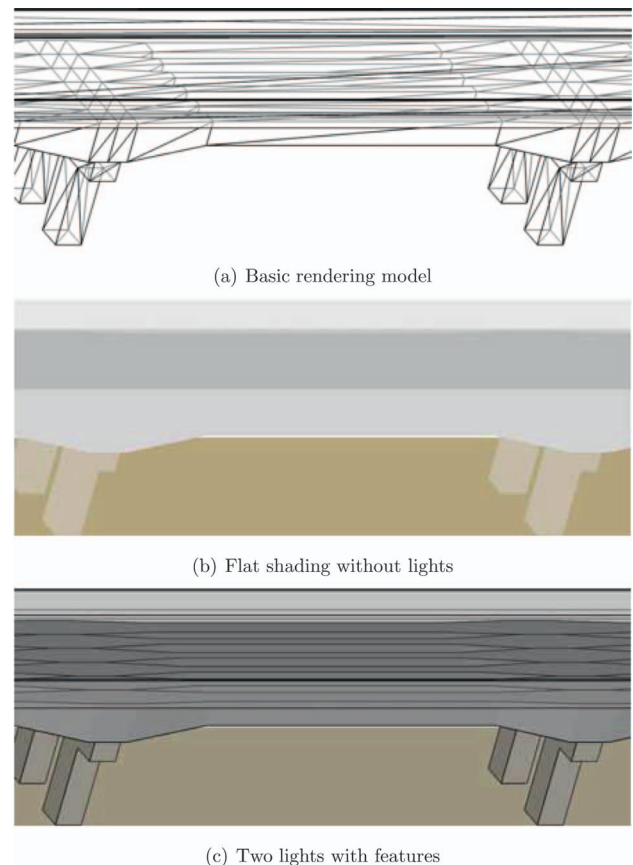
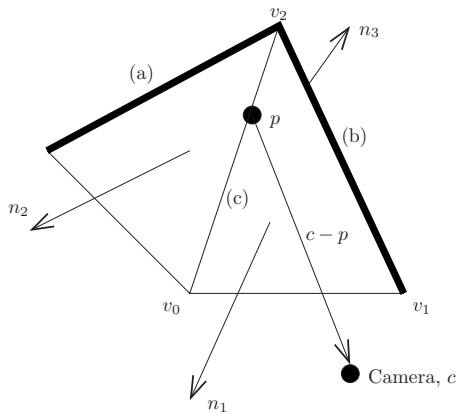


Fig. 5. (Color) Choice of rendering techniques can improve the visual definition of the bridge



**Fig. 6.** (a and b) Edges are shared by front and back facing polygons and are considered silhouette edges. (c) Edge is shared by two front facing polygons and is not classified as a silhouette edge.

shows varying girder dimensions near the bents. Girder spacing and tapered dimensions become more prominent, giving the viewer more realistic visual feedback about the bridge geometry.

### Feature Edges

While lighting gives a sense of shape and orientation to the bridge visualization, features such as sharp edges can still be difficult to discern when viewed at specific angles. To this end, the visualization system utilizes two techniques to draw feature edges: sharp edge highlighting and silhouette edge detection (Hertzmann and Zorin 2000).

The first feature technique, similar to Ohtake and Seidel (2004), highlights important view-independent features of the bridge. The basic idea is to draw lines along the contours of greatest local maximum and minimum curvatures on the surface of the mesh. Due to the assumption of flat bridge surfaces, the following simplification is made: sharp edges in the mesh can be found by comparing the angle between two faces incident to an edge. If this angle is greater than a constant (set to  $80^\circ$  in this visualization system), the edge is considered sharp. This test finds the edges that have a large angle between normal vectors on adjacent faces, resulting in highlighting of only the sharp edges of bridge components. This can be seen in Fig. 5(c), where outlining gives a clear indication of transverse girder spacing while not overcrowding the image with outlines of dull edges owing to tapers and haunches near the supports.

The second technique, silhouette edge detection, can improve the visual quality by finding the outline of the bridge, which is view dependent. A silhouette edge is formed when the normal vectors of two adjacent faces ( $n_1$  and  $n_2$ ) are in opposite directions from the viewer

$$[n_1 \cdot (c - p)] \times [n_2 \cdot (c - p)] < 0 \quad (1)$$

where  $c = (x_c, y_c, z_c)$  is the viewer's camera position and  $p = [x, y, f(x, y)]$  is a point on the edge, as shown in Fig. 6. Silhouette detection is done in a two-step process. The first step cycles over the faces of the mesh, classifying them as either front facing or back facing. The second step cycles over the edges of the mesh, drawing the edges that have adjacent front and back faces. To cut down on redundant information and improve efficiency of the entire feature edge drawing process, the sharp edge test is performed after the first step of the silhouette test such that the mesh edge information is processed only once.

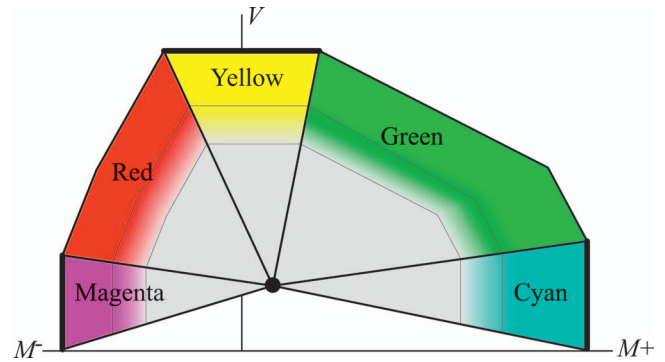


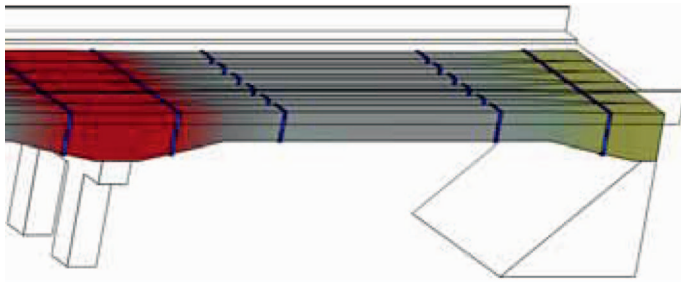
**Fig. 7.** (Color) Color mapping of reliability indices to modes of most probable girder failure: positive moment (cyan); combined positive moment and shear (green); shear (yellow); combined negative moment and shear (red); and negative moment (magenta). Gray indicates regions where the probability of failure is less than the user-specified level.

### Bridge Rating Visualization

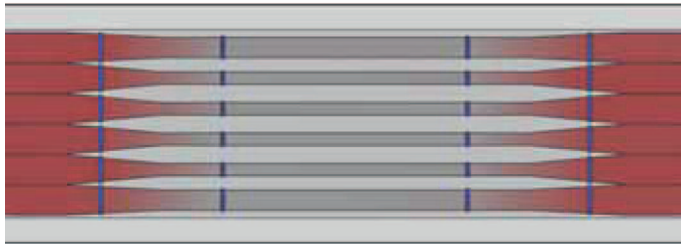
The visualization of bridge rating is based on the color map shown in Fig. 7, where there are five modes of girder failure which correlate to the combined moment-shear rating methodology shown in Fig. 1(c). Magenta and cyan indicate failure due to negative and positive bending moments, respectively, while yellow indicates shear failure. Failure under combined shear and negative (positive) moment is indicated by red (green). For reinforced concrete highway bridges designed according to standard specifications, the most likely modes of failure will be positive moment (cyan) near midspan locations and combined shear/negative moment (red) near continuous interior supports. When the rating for single force effects [Figs. 1(a and b)], red and green fall out of the color mapping, transforming Fig. 7 in to a magenta-yellow-cyan rectangle.

As shown in Fig. 7, there are three color regions for each mode of girder failure. When the critical moment-shear demand due to vehicle live load falls within the gray region, the girder cross section satisfies the inventory rating condition of performing safely indefinitely (AASHTO 2003). For the evaluation method shown in Fig. 1(c), the inventory condition corresponds to  $\beta$  values greater than 3.5. On the other hand, solid coloring of one of the five failure modes indicates the section does not satisfy the operating rating condition (AASHTO 2003) or the maximum allowable moment-shear interaction effect is exceeded. This condition corresponds to  $\beta$  values less than 2.5. Portions of the bridge girders that do not meet this operating rating condition may require immediate repair or load posting of the affected bridge. The color of regions between the inventory and operational rating thresholds is obtained by linear blending of the associated failure color and gray.

Bridge rating values are global over the entire length of a girder, i.e., the color codings are independent of the faces and edges of the bridge mesh. Limitations in hardware make it necessary to treat the transition region uniquely. As a result, a different approach must be taken to visualize the rating calculations. To this end, the girder mesh is subdivided along the region boundaries. Also, to take into account global bridge rating information, the color coding from one critical section is carried over to the next bridge span. In the absence of more detailed information, the color codings between two adjacent critical sections along a



(a) Hiding auxiliary bridge features of an end span.



(b) Looking from above the bridge at a center span.

**Fig. 8.** (Color) Orthographic views with the bridge rating visualization enabled

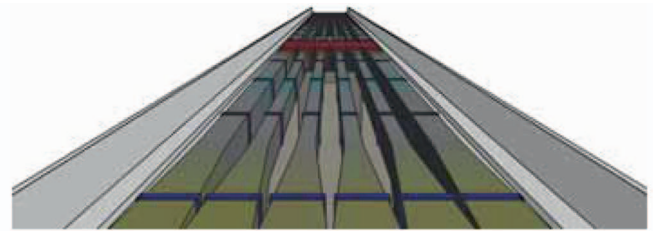
girder are obtained by linear blending between two colors of the sections. Two views of the bridge rating visualization are shown in Fig. 8, with blending between critical bridge sections close to interior and end supports and those located near midspan, where there is a lower probability of failure.

### Future Extensions

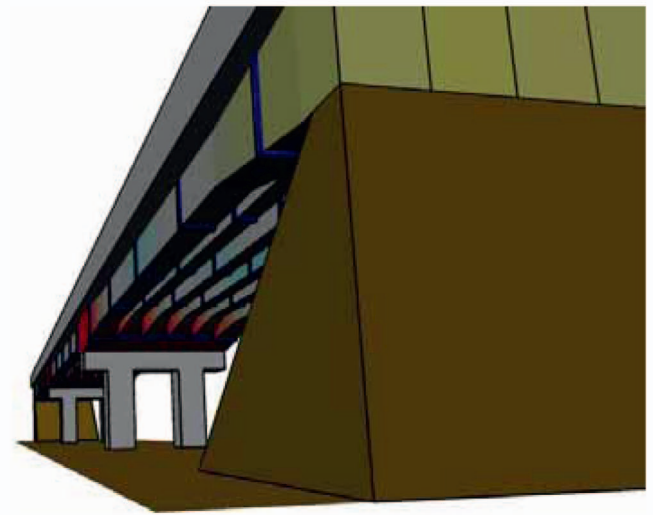
Several extensions of the bridge rating software are possible due to the intentional loose coupling of the analysis, rating, and visualization modules. The incorporation of nonlinear behavior to account for vehicle overload conditions is straightforward using the state-of-the-art finite-element formulations and constitutive models available in OpenSees (Mazzoni et al. 2006). In addition, extensions to emergent rating methodologies are envisioned by drawing upon the finite-element reliability modules that have been implemented in OpenSees (Haukaas and Der Kiureghian 2007).

To enhance the physical realism of the structural analysis, moving vehicles will be added to the visualization along with stress contours and mesh deformations. As computing power increases, these response quantities along with bridge rating information can be viewed in real time as part of health monitoring applications using weigh-in-motion data rather than notional configurations of axle weights. In addition, recent advances in tensor field analysis (Delmarcelle and Hesselink 1994; Hesselink et al. 1997; Zheng and Pang 2004; Zheng et al. 2005) and visualization (Zheng and Pang 2003; Zhang et al. 2007; Hotz et al. 2004) have the potential of enriching the visualization system with stress tensor rendering at discrete points on a girder cross section.

In addition to the orthographic bridge views shown in Figs. 5 and 8, the visualization system is capable of rendering perspective views of a bridge. This makes the system readily extensible to bridge rating applications involving virtual and augmented reality. Fig. 9(a) shows rating colors viewed down the bridge from a



(a) Bridge rating visualization looking down a bridge.



(b) Looking up from the ground at the underside of a bridge

**Fig. 9.** (Color) Perspective views with the bridge rating visualization enabled

driver's point of view while Fig. 9(b) shows the view point of a field engineer inspecting the underside of a bridge for signs of damage, e.g., concrete cracking, at girder locations where the rating calculations indicate a high likelihood of failure. Further extensions to earthquake reconnaissance using augmented reality (Kamat and El-Tawil 2007) are also possible using the bridge rating visualization system presented in this paper.

Recent advances in the fields of computer graphics, scientific visualization, and geometric modeling can be applied to improve various aspects of the bridge rating visualization system presented in this paper. One such development that can have an impact on the efficiency and speed of the bridge rating system presented in this paper and 3D visualization applications in civil engineering in general is the use of graphics processing units (GPU). The GPU-based algorithms typically outperform their central processing units counterparts by an order of magnitude and have already made significant impacts in computer graphics applications such as medical imaging (Petrovic et al. 2007), crack analysis (Wilson and Brannon 2005), terrain visualization (Losasso and Hoppe 2004), scientific computing (Bolz et al. 2003), and volume rendering (Georgii and Westermann 2006). This makes it feasible to interactively display large 3D and time-varying data sets. It is envisioned that GPUs will thus play an important role in real-time 3D visualization of bridge rating, health monitoring, and virtual and augmented reality applications.

### Conclusions

Graphical 3D visualization of RCDG bridge ratings provides important information regarding the possible modes of girder failure

under combined moment-shear force effects. By visualizing the comparison of demand with capacity, engineers can readily see the portions of a bridge that are in need of repair, which may not be obvious from viewing only the extreme force effects, particularly when considering moment-shear interaction. The use of general purpose finite-element analysis in OpenSees, as well as the extensible OpenGL graphics library, allows the system to be adapted to other bridge types. In addition, the reliance on a scripting language for analysis and rating allows an engineer to experiment with emergent rating methodologies without making significant changes to the software core. Shading and feature edge highlighting enhance the visualization and provide a realistic representation of important bridge features.

## Acknowledgments

The writers thank the Oregon Department of Transportation for sponsoring the development of this bridge rating visualization system. The views expressed in this paper do not necessarily reflect those of the sponsoring agency.

## References

- AASHTO (2003). *Manual for condition evaluation and load and resistance factor rating (LRFR) of highway bridges*, American Association of State Highway and Transportation Officials, Washington, D.C.
- Akgül, F., and Frangopol, D. M. (2004). "Bridge rating and reliability correlation: Comprehensive study for different bridge types." *J. Struct. Eng.*, 130(7), 1063–1074.
- Bathe, K. J. (1996). *Finite element procedures*, Prentice-Hall, Upper Saddle River, N.J.
- Bolz, J., Farmer, I., Grinspun, E., and Schröder, P. (2003). "Sparse matrix solvers on the GPU: Conjugate gradients and multigrid." *ACM Trans. Graphics*, 22(3), 917–924.
- Booch, G., Rumbaugh, J., and Jacobson, I. (1998). *The unified modeling language user guide*, Addison-Wesley, Reading, Mass.
- Chung, W., and Sotelino, E. D. (2006). "Three-dimensional finite element modeling of composite girder bridges." *Eng. Struct.*, 28(1), 63–71.
- Delmarcelle, T., and Hesselink, L. (1994). "The topology of symmetric, second-order tensor fields." *Proc., IEEE Visualization '94*, IEEE Computer Society Press, Los Alamitos, Calif., 140–147.
- Foley, J. D., van Dam, A., Feiner, S. K., and Hughes, J. F. (1996). *Computer Graphics: Principles and Practices in C*, 2nd Ed., Addison-Wesley, Reading, Mass.
- Georgii, J., and Westermann, R. (2006). "A generic and scalable pipeline for GPU tetrahedral grid rendering." *IEEE Trans. Vis. Comput. Graph.*, 12(5), 1345–1352.
- Gottschalk, S., Lin, M. C., and Manocha, D. (1996). "OBBTree: A hierarchical structure for rapid interference detection." *Proc., Computer Graphics*, ACM, New York, 171–180.
- Haukaas, T., and Der Kiureghian, A. (2007). "Methods and object-oriented software for FE reliability and sensitivity analysis with application to a bridge structure." *J. Comput. Civ. Eng.*, 21(3), 151–163.
- Hertzmann, A., and Zorin, D. (2000). "Illustrating smooth surfaces." *Proc., 27th Annual Conf. on Computer Graphics and Interactive Techniques*, Addison-Wesley, Reading, Mass., 517–526.
- Hesselink, L., Levy, Y., and Lavin, Y. (1997). "The topology of symmetric, second-order 3D tensor fields." *IEEE Trans. Vis. Comput. Graph.*, 3(1), 1–11.
- Higgins, C., et al. (2004). "Reliability based assessment methodology for diagonally cracked conventionally reinforced concrete deck girder bridges: An integrated approach." *Rep. No. SPR 350*, Oregon Dept. of Transportation, Salem, Ore.
- Higgins, C., Daniels, T. K., Rosowsky, D. V., Miller, T. H., and Yim, S. C. (2005). "Assessment and risk ranking of conventionally reinforced concrete bridges for shear." *J. Transp. Res. Board*, 1928, 110–117.
- Hotz, H., Feng, L., Hagen, H., Hamann, B., Joy, K., and Jeremic, B. (2004). "Physically based methods for tensor field visualization." *Proc., IEEE Visualization 2004*, IEEE Computer Society, Washington, D.C., 123–130.
- Hughes, T. J. R. (1987). *The finite element method*, Prentice-Hall, Englewood Cliffs, N.J.
- Hutchinson, T. C., Kuester, F., and Phair, M. E. (2007). "Sketching finite-element models within a unified two-dimensional framework." *J. Comput. Civ. Eng.*, 21(3), 175–186.
- Kamat, V. R., and El-Tawil, S. (2007). "Evaluation of augmented reality for rapid assessment of earthquake-induced building damage." *J. Comput. Civ. Eng.*, 21(5), 303–310.
- Kamat, V. R., and Martinez, J. C. (2001). "Visualizing simulated construction operations in 3D." *J. Comput. Civ. Eng.*, 15(4), 329–337.
- Losasso, F., and Hoppe, H. (2004). "Geometry clipmaps: Terrain rendering using nested regular grids." *ACM Trans. Graphics*, 23(3), 769–776.
- Mazzoni, S., McKenna, F., Scott, M. H., and Fenves, G. L. (2006). *Open system for earthquake engineering simulation user command-language manual—Version 1.7.3*, University of California, Berkeley, Calif., (<http://opensees.berkeley.edu/OpenSees/manuals/usennannual/>) (November 30, 2007).
- McKenna, F., Fenves, G. L., and Scott, M. H. (2000). *Open system for earthquake engineering simulation*, University of California, Berkeley, Calif., (<http://opensees.berkeley.edu>) (November 30, 2007).
- Minervino, C., Sivakumar, B., Moses, F., Mertz, D., and Edberg, W. (2004). "New AASHTO guide manual for load and resistance factor rating of highway bridges." *J. Bridge Eng.*, 9(1), 43–54.
- Ohtake, Y., and Seidel, E. (2004). "Ridge-valley lines on meshes via implicit surface fitting." *ACM Trans. Graphics*, 23, 609–612.
- Oregon Department of Transportation (ODOT). (2002). "Oregon's bridges 2002." Oregon Department of Transportation, Salem, Ore., ([http://www.odot.state.or.us/tsbbridgepub/PDFs/Senate\\_05\\_16.02.pdf](http://www.odot.state.or.us/tsbbridgepub/PDFs/Senate_05_16.02.pdf)) (November 30, 2007).
- Oregon Department of Transportation (ODOT). (2004). *Bridge design and drafting manual (BDDM)*, Oregon Department of Transportation, Salem, Ore.
- Ousterhout, J. K. (1994). *Tcl and the Tk toolkit*, Addison-Wesley, Reading, Mass.
- Petrovic, V., Fallon, J., and Kuester, F. (2007). "Visualizing whole-brain DTI tractography with GPU-based tuboids and LoD management." *IEEE Trans. Vis. Comput. Graph.*, 13(6), 1488–1495.
- Scoggins, L. (2007). "3-D finite element modeling in OpenSees for bridge live-load girder distribution factors." MS thesis, Oregon State Univ., Corvallis, Ore.
- Shreiner, D., Woo, M., Neider, J., and Davis, T. (2007). *OpenGL(R) programming guide: The official guide to learning OpenGL(R), version 2.1*, Addison-Wesley, 6th Ed., Reading, Mass.
- Stasko, J., and Zhang, E. (2000). "Focus+context display and navigation techniques for enhancing radial, space-filling hierarchy visualizations." *Proc., IEEE Symp. on Information Visualization 2000*, IEEE Computer Society, New York, N.Y., 57–65.
- Stewart, M. G., Rosowsky, D. V., and Val, D. (2001). "Reliability-based bridge assessment using risk-ranking decision analysis." *Struct. Safety*, 23, 397–405.
- Turan, O. T., Higgins, C., and Rosowsky, D. V. (2008). "Statistical modeling of coupled shear-moment resistance for RC bridge girders." *J. Bridge Eng.*, 13(4), 351–361.
- van der Zijp, J. (2007). "Fox toolkit." (<http://www.fox-toolkit.org/>) (November 30, 2007).
- Welch, B. B. (2000). *Practical programming in Tcl and Tk*, 3rd Ed., Prentice-Hall, Upper Saddle River, N.J.
- Wilson, A., and Brannon, R. (2005). "Exploring 2D tensor fields using stress nets." *Proc., Visualization 2005—VIS'05*, IEEE Computer Society, Washington, D.C.

- Zhang, E., Hays, J., and Turk, G. (2007). "Interactive tensor field design and visualization on surfaces." *IEEE Trans. Vis. Comput. Graph.*, 13(1), 94–107.
- Zheng, X., and Pang, A. (2003). "HyperLIC." *Proc., IEEE Visualization '03*, IEEE Computer Society, Washington, D.C., 249–256.
- Zheng, X., and Pang, A. (2004). "Topological lines in 3D tensor fields." *Proc., Visualization '04*, IEEE Computer Society, Washington, D.C., 313–320.
- Zheng, X., Parlett, B., and Pang, A. (2005). "Topological structures of 3D tensor fields." *Proceedings IEEE Visualization 2005*, IEEE Computer Society, Washington, D.C., 551–558.
- Zienkiewicz, O. C., and Taylor, R. L. (2000). *The finite element method: Volume 1, the basis*, 5th Ed., Butterworth-Heinemann, Stoneham, Mass.